2010 American Control Conference
Marriott Waterfront, Baltimore, MD, USA
June 30-July 02, 2010

Modal actuation for high bandwidth nano-positioning

J.R. van Hulzen, G. Schitter, P.M.J. Van den Hof and J. van Eijk

Abstract— **In high speed AFMs the vertical axis of the sample positioning stage requires high bandwidth feedback control. In these systems the dynamics of the piezoelectric actuator, its support structure and load play a dominant role in the design of the feedback loop. System performance can be increased by avoiding the excitation of resonant modes of the piezoelectric actuator by modal actuation. In this approach, the piezoelectric actuator is modified to render modes close to the controller bandwidth uncontrollable. Due to its static hardware implementation robustness issues may emerge due to varying loads used for AFM imaging. This paper focusses on performance robustness of modal filters due to load variation.**

I. INTRODUCTION

Piezoelectric actuators are used in applications where high precision position is required over a relatively short range. A typical example of such an application is the atomic force microscope (AFM) [1]. In an AFM the topography of a sample is imaged on a nanometer scale by measuring the deflection of a cantilever which is in contact with the sample surface through a sharp protruding tip (see [2] for an overview). To avoid damage to sample or tip, the cantilever deflection is regulated by tracking the sample topography using a feedback control system.

In high speed AFMs, the bandwidth of the vertical axis positioning system is a limiting factor. In recent developments, improvements to this system have been proposed. The mechanical design has been improved by making the scanner smaller and more rigid [3],[4] and by balancing of the vertical stage by using two counteracting actuators [5]. Model-based controllers for the lateral and vertical axis have been implemented [4],[6]-[10] and have been shown to improve performance.

A common problem in the design of such control systems is the excitation of resonant modes which are close to the controller bandwidth [11],[12]. A possible solution to this problem is the application of a modal actuation [13]. A modal pre-filter can be used to drive only a subset of modes while rendering others uncontrollable. Modal filtering has been applied in piezoelectric actuated systems successfully by shaping the driving electrode by etching [14] by application of a porous distributed electrode using a electrode with a honeycomb motif [15], [16]. Modal filters based on arrays of individual piezoelectric transducers have been reported in [17], [18]. A drawback of the hardware implementation of a modal actuator is its inflexibility. In applications where the system dynamics are subject to change due to the introduction of additional loads this may lead to unwanted oscillations or instability.

This paper focusses on the application of modal actuation on piezoelectric tube scanners used in AFMs. The goal is to shape the dynamics of the piezoelectric actuator by shifting the anti-resonant modes towards resonant modes that are close to the system bandwidth.

The paper is organized as follows. In Section II, the dynamics of the piezoelectric tube actuator are derived. In Section III the design of a modal actuator is discussed. In Section IV, the modal actuation approach is verified experimentally. Finally, conclusions are given in Section V.

II. MODAL ACTUATION

A piezoelectric actuator consists of a stiff ceramic material which expands due to forces generated by the piezoelectric effect. In [19] and [20] dynamical models of piezoelectric actuators are proposed. In these models, axial vibration in the piezo material is modeled using a partial differential equation. The load is assumed to be a rigid mass which is mounted on the free end of the actuator.

To show that a piezoelectric actuator can be transformed into a modal actuator, where specific modes of the axial dynamics are excited while other are suppressed, it is necessary to solve the differential eigenvalue problem and show that the spatial solutions or natural modes are orthogonal to each other. If this is the case the natural modes can be excited independently and a solution can be decomposed into a linear combination of modes.

A. Axial vibration of a piezoelectric tube scanner

The vertical axis of a tube scanner is modeled under the assumptions that there is neither bending nor shear and that the tube retains its shape during extension (see [21] for an overview of beam and shell theory). The axial displacement $u(x,t)$ in the piezo material is modeled using a second order partial differential equation

$$EA\frac{\partial^2 u(x,t)}{\partial x^2} = A\rho\frac{\partial^2 u(x,t)}{\partial t^2};\ 0 < x < L \qquad (1)$$

in which L is the length of the material, E is the modulus of elasticity, A the effective area of the lateral cross section and ρ the density. The actuator is connected to mechanical ground at $x = 0$ by a spring k which models the compliance

This work is part of a project on Model-based subnano-positioning control systems for high-end professional equipment and microsystems manipulation sponsored by the Delft Center for Mechatronics and Microsystems.

J.R. van Hulzen, P.M.J. Van den Hof are with the Delft Center for Systems and Control, Delft University of Technology, Mekelweg 2, 2628 CD Delft, The Netherlands, J.R. van Hulzen, G. Schitter and J. van Eijk are with the Precision and Microsystems Engineering Department, Delft University of Technology, Mekelweg 2, 2628 CD Delft, The Netherlands, j.r.vanhulzen@tudelft.nl

of the support and loaded by a rigid mass m_l at $x = L$. The boundary conditions are

$$EA\frac{\partial u(x,t)}{\partial x} = kU(x),\ x = 0, \tag{2}$$

$$-EA\frac{\partial u(x,t)}{\partial x} = m_l\frac{\partial^2 u(x,t)}{\partial t^2},\ x = L. \tag{3}$$

Under the assumption that the system executes synchronous motion [22] the solutions of (1)-(3) can be separated into a function of the spatial variable x and function of time t and can be described as

$$u_i(x,t) = U_i(x)\cos(\omega_i t - \alpha_i) \tag{4}$$

where $u_i(x,t)$ are the natural motions with $U_i(x)$ as the mode shapes of the natural modes and ω_i as the natural frequencies which are obtained by solving the differential eigenvalue problem. Using (4), Equations (1)-(3) transform into

$$-EA\frac{d^2U_i(x)}{dx^2} = \omega^2\rho AU_i(x),\ 0 < x < L, \tag{5}$$

$$EA\frac{dU_i(x)}{dx} = kU_i(x),\ x = 0, \tag{6}$$

$$EA\frac{dU_i(x)}{dx} = \omega^2 m_l U_i(x),\ x = L. \tag{7}$$

Assuming natural modes in the form

$$U_i(x) = \cos\left(\frac{\lambda_i}{L}x - \beta_i\right), \tag{8}$$

with parameters λ_i and β_i given by

$$\tan(\lambda_i) + \tan(\lambda_i)\frac{kL}{EA}\frac{m_l}{\rho AL} = \frac{kL}{EA}\frac{1}{\lambda_i} - \frac{m_l}{\rho AL}\lambda_i \tag{9}$$

and

$$\tan(\beta_i) = \frac{kL}{EA}\frac{1}{\lambda_i}, \tag{10}$$

the natural frequencies ω_i can be derived using

$$\omega = \frac{\lambda}{L}\sqrt{\frac{E}{\rho}}. \tag{11}$$

To show that the separate modes can be excited independently it is necessary to derive the orthogonality conditions.

B. Orthogonality

To derive the orthogonality conditions, two solutions $U_a(x)$ and $U_b(x)$ satisfying

$$-EA\frac{d^2U_a(x)}{dx^2} = \omega_a^2 A\rho U_a(x),\ \ 0 < x < L, \tag{12}$$

$$-EA\frac{d^2U_b(x)}{dx^2} = \omega_b^2 A\rho U_b(x),\ \ 0 < x < L \tag{13}$$

are compared. Multiplication of (12) with $U_b(x)$ and integration over x yields

$$-EA\int_0^L U_b(x)\frac{d^2U_a(x)}{dx^2}dx = \omega_a^2\rho A\int_0^L U_b(x)U_a(x)dx \tag{14}$$

Integrating the left hand side by parts yields

$$EA\int_0^L U_b(x)\frac{d^2U_a(x)}{dx^2}dx = EA\,U_b(x)\frac{dU_a(x)}{dx}\bigg|_0^L - EA\int_0^L \frac{dU_b(x)}{dx}\frac{dU_a(x)}{dx}dx. \tag{15}$$

Using the boundary conditions (6) and (7) it follows that

$$EA\,U_b(x)\frac{dU_a(x)}{dx}\bigg|_0^L = \omega_a^2 m_l U_b(L)U_a(L) - kU_b(0)U_a(0). \tag{16}$$

Inserting (15) and (16) into (14) yields

$$EA\int_0^L \frac{dU_b(x)}{dx}\frac{dU_a(x)}{dx}dx + kU_b(0)U_a(0) = \omega_a^2\left\{\rho A\int_0^L U_b(x)U_a(x)dx + m_l U_b(L)U_a(L)\right\}. \tag{17}$$

Multiplication of (13) with $U_a(x)$, integrating over x and repeating the same steps yields

$$EA\int_0^L \frac{dU_a(x)}{dx}\frac{dU_b(x)}{dx}dx + kU_a(0)U_b(0) = \omega_b^2\left\{\rho A\int_0^L U_a(x)U_b(x)dx + m_l U_a(L)U_b(L)\right\} \tag{18}$$

then, subtracting (17) from (18) we have

$$(\omega_b^2 - \omega_a^2)\left\{\rho A\int_0^L U_a(x)U_b(x)dx + m_l U_a(L)U_b(L)\right\} = 0,$$

which leads to the orthogonality relations

$$\rho A\int_0^L U_a(x)U_b(x)dx + m_l U_a(L)U_b(L) = \mu_a\delta_{ab} \tag{19}$$

$$EA\int_0^L \frac{dU_a(x)}{dx}\frac{dU_b(x)}{dx}dx + kU_a(0)U_b(0) = \omega_a^2\mu_a\delta_{ab} \tag{20}$$

in which $a, b = 1, 2, ...$ and δ_{ab} is the Kronecker delta function. The parameter μ_a is a scaling factor often referred to as the modal mass and is given by

$$\mu_a = A\rho\int_0^L U_a^2(x)dx + m_l U_a^2(L).$$

Inserting (8) yields the expression

$$\mu_a = \rho A\int_0^L \cos^2\left(\lambda_a\frac{x}{L} - \beta_a\right)dx + m_l\cos^2(\lambda_a - \beta)$$

then, using (9),(10) and (11) it follows that

$$\mu_a = \tfrac{1}{2}\rho AL + \tfrac{1}{2}m_l\cos^2(\lambda_a - \beta_a) + \tfrac{1}{2}\frac{EA}{kL}\rho AL\sin^2\beta_a.$$

The orthogonality conditions and the modal mass enable modal decomposition of the system.

C. Response to external excitation

To derive the response to external excitation (1) is extended to

$$EA\frac{\partial^2 u(x,t)}{\partial x^2} + f(x,t) = A\rho\frac{\partial^2 u(x,t)}{\partial t^2};\ 0 < x < L. \quad (21)$$

in which $f(x,t)$ is the net-force generated by the piezoelectric effect per unit length. To derive the transfer function of the system in modal form, a solution in the form

$$u(x,t) = \sum_{i=1}^{\infty} U_i(x)q_i(t) \quad (22)$$

is used. Inserting (22) into (21), multiplying both sides with $U_a(x)$, integrating over x and using the orthogonality relations (19), (20) it follows that

$$\ddot{q}_i(t) + \omega_i^2 q_i(t) = \mu_i^{-1}\int_0^L U_i(x)f(x,t)dx$$

Without any restriction we can assume $f(x,t) = F(x)cos\omega t$ to obtain

$$u(x,t) = \sum_{i=1}^{\infty}\frac{\int_0^L U_i(x)F(x)dx}{\mu_i(\omega_i^2 - \omega^2)}U_i(x)\cos\omega t$$

and the transfer function from force to extension is

$$P(x,\omega) = \sum_{i=1}^{\infty}\frac{g_i}{\mu_i(\omega_i^2 - \omega^2)}U_i(x)$$

with the modal gain g_i defined as

$$g_i = \int_0^L U_i(x)F(x)dx$$

D. Modal actuation using sectioned electrodes

In a standard piezoelectric tube actuator the inner and outer electrodes are continuous. To discretize the actuator for spatially distributed excitation, the live electrode is divided into sections leaving the ground electrode unaltered, see Fig. 5b. The number of sections depends on the width of the separation between the sections which influences the efficiency of the piezo. Each section has an uniform electrode which means that the force generated over a section can be modeled as as set of two equal forces acting on the section boundaries. With this assumption $F(x)$ can be written as

$$F(x) = \sum_{j=1}^{n+1} g_j\big(\delta(x - x_j) - \delta(x - x_{j+1})\big)$$

where δ is the dirac function, n is the number of sections, g_j is the section gain and x_j the coordinate of the lower boundary of a section. The expression for modal gain changes into

$$g_i = \int_0^L U_i(x)F(x)dx = \sum_{j=1}^{n} g_j\big(U_i(x_{j+1}) - U_i(x_j)\big)$$

with $U_i(x) = \cos\left(\lambda_i x/L - \beta_i\right)$ we have

$$g_i = \sum_{j=1}^{n} g_j\left(\cos\left(\lambda_i\frac{x_{j+1}}{L} - \beta_i\right) - \cos\left(\lambda_i\frac{x_j}{L} - \beta_i\right)\right)$$

If n modes are selected by choosing a set of modal gains g_i we can solve this set of equations to obtain the required section gains g_j. This gives the designer the freedom to shift the anti-resonances of the actuator dynamics towards a specified set of resonant modes which enables selective excitation of individual modes while rendering others uncontrollable.

E. Design of modal actuator

The design a modal actuator can be based on modeling as well as on experimental data. Once the frequency response functions of the system are derived, modal actuation can be based least squares optimization using a selected set of peak gains, on hand tuning by combining sections into larger sets or on the mode shape of a simple configuration. A good starting point in the latter approach is $g_j = \cos(\lambda x_j/L)$ with $\lambda = \frac{\pi}{2}$ as an initial guess. The optimal λ is found shifting the anti resonance between the first and second mode towards the second mode.

A model of the system shown in Fig. 5 based on material constants is shown in Fig. 1. In this model the connection between actuator and mount is assumed to be rigid. The dynamics of the sections $1-5$ shown in Fig. 1 indicate that the individual sections are non-collocated while the sections driven together act as a collocated system. A prerequisite for this is that the separation between the electrodes is very small and that all sections are driven using the same voltage.

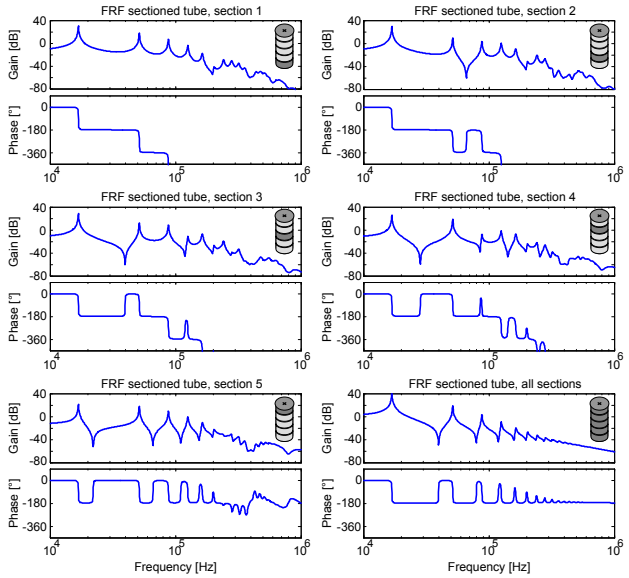

Fig. 1. Model of axial dynamics ($F_i \rightarrow z$) of a sectioned piezoelectric tube with a stiff connection between tube and mechanical ground.

The influence of a compliant actuator support ($k = 1\times10^7$ N/m) is shown in Fig. 2. In this case the first resonant mode has shifted from 17 kHz to 7.5 kHz. From Fig. 2 it is clear that the order of resonance and anti resonant modes has changed. Also, in contrast with the rigid-mount case shown in Fig. 1, the system with all sections driven with the same

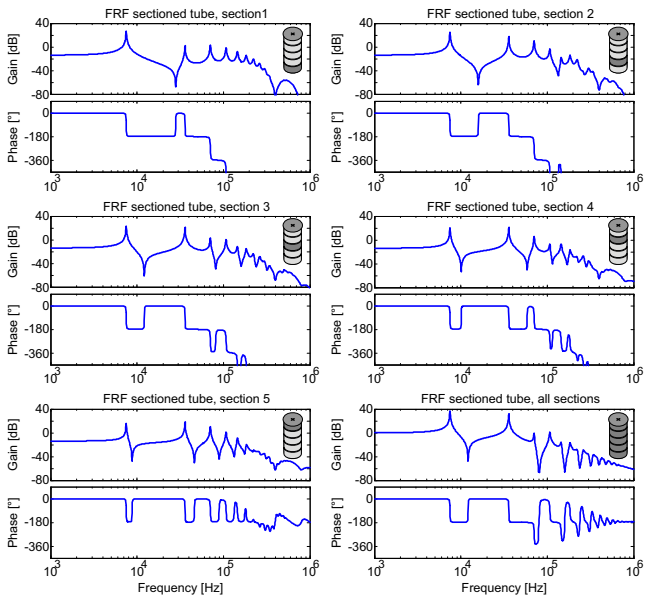

Fig. 2. Model of axial dynamics ($F_i \rightarrow z$) of a sectioned piezoelectric tube with a compliant connection between tube and mechanical ground.

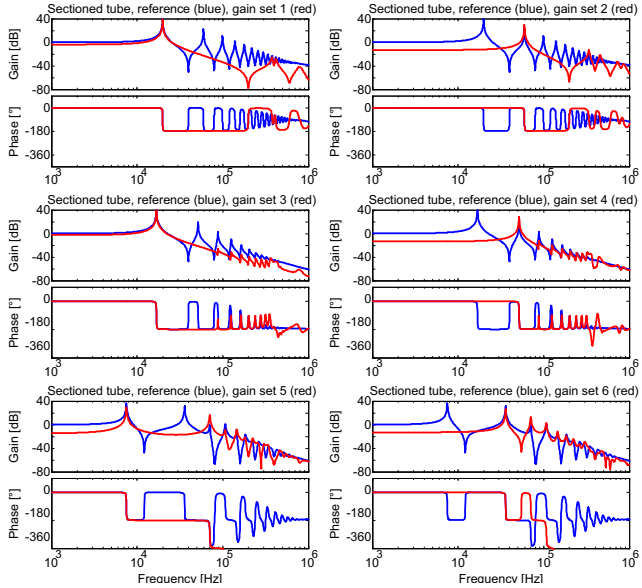

Fig. 3. FRF of piezoelectric tube with section gains set to 1 (blue) and section gains set to modal gains of first, second and third mode (red).

voltage is no longer collocated. This is due to the fact that the force acting on the lower boundary is taken into account.

In Fig. 3, designs for modal actuators fitting three load condition are shown: unloaded (set 1-2), loaded by a rigid mass (set 3-4) and a combination of a rigid mass load and a compliant actuator mount (set 5-6). In all three cases a design for cancelation of the second and higher modes (set 1,3 and 5) is compared to a design canceling the first, third and higher modes (set 2,4 and 6). The gain sets listed in Table I are derived by curve fitting a cosine function in the form $\cos(\lambda x_j/L - \beta)$ to the modal data obtained from the models of each specific load condition.

In the unloaded case using gain set 1, the cancelation up to the tenth mode is very good. Above the tenth mode there is some spill over due to spatial aliasing. Gain set 2 cancels the first, third and higher order modes but also reduces the static gain to 23% of its original value. Comparing gain set 3 with gain set 5 in Table I and Fig. 3 it follows that the optimal gain set in the compliant mount case yields a lower static gain due to the fact that gain set 5 has negative values.

The effect of modal actuation on the static gain of an actuator with varying load conditions is shown in Fig. 4. In all cases the application of modal actuation reduces the static gain of the actuator. However, comparing the static gain of a system with a rigid mass with the case where the actuator is unloaded it follows that an introduced load increases the static gain. The reason for this is that the modes used for cancelation in case of an actuator with load has a smaller slope than the case without load. In contrast a compliant actuator support reduces static gain.

TABLE I

MODAL ACTUATOR GAIN SETS

set	g_1	g_2	g_3	g_4	g_5	m_l	k
1	1.00	0.90	0.72	0.46	0.16	0	∞
2	-0.90	-0.16	0.72	1.00	0.46	0	∞
3	1.00	0.93	0.79	0.59	0.36	.64 g	∞
4	-0.96	-0.37	0.46	1.00	0.92	.64 g	∞
5	1.00	0.73	0.25	-0.29	-0.75	.64 g	10^7 N/m
6	-0.90	-0.19	0.66	1.00	0.55	.64 g	10^7 N/m

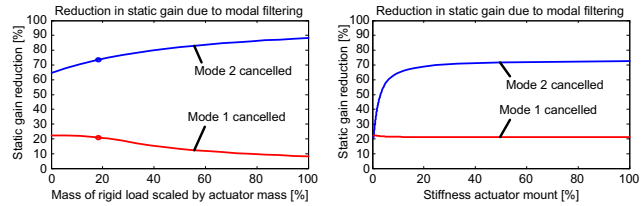

Fig. 4. Reduction in static gain due to the application of modal filtering as a function of load conditions with changes due to different rigid masses (left) and changes due to a compliant ($10^7 N/m = 100\%$) actuator mount (right).

III. EXPERIMENTAL VERIFICATION

To verify the modal actuation approach, the outer electrode of a commercially available piezoelectric tube actuator (PT130.20, Physik Instrumente, Karlsruhe, Germany) was segmented into five sections of equal length using a lathe. The sectioned tube was excited using a set of five custom piezo amplifiers with a configurable gain.

In Fig. 5 an overview of the experimental setup is presented. The actuator has a length $L = 30\ mm$, an inner diameter of $d_i = 9\ mm$, an outer diameter $d_o = 10\ mm$ and a lateral cross section $A = 15\ mm^2$. The ceramic material of the tube is PIC 151, which has a density $\rho = 7.76 \times 10^3\ kg/m^3$ and a modulus of elasticity $c_{13}^D = 44\ GPa$ and $c_{13}^E = 64\ GPa$ depending on the electrical boundary conditions.

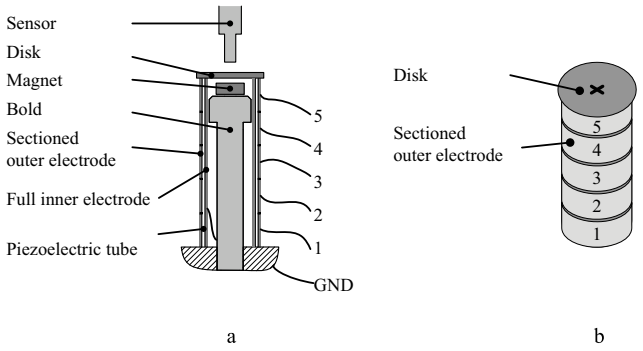

Fig. 5. Overview of the experimental setup of the sectioned piezoelectric tube with a vertical cross section (a) and an overview of the sections (b).

Loads in the form of standard AFM sample carriers (usually a thin steel disk) are held into place using a small magnet bonded to a M4 bolt which is connected to the base. The magnet and the load are in close proximity of each other but not in contact. The tube rests on an aluminum block under a pre-load force generated by the magnet and is not bonded to allow radial expansion.

The actuator is loaded by a standard steel ($\rho = 7.8 \times 10^3$ kg/m^3, $E = 200$ GPa) sample carrier with radius $r = 6$ mm, thickness $h = 0.72$ mm and a mass $m_l = 0.64$ g. The lowest resonant mode of the sample carrier can be derived using [21]

$$f = \lambda_{ij}^2 \frac{h}{2\pi r^2} \sqrt{\frac{E}{12\rho(1-\nu^2)}}$$

which with $\lambda_{01}^2 = 4.977$ results in 24 kHz. Therefore it can be concluded that the lowest resonant mode of the sample carrier is in the same range as the low order modes of the piezoelectric actuator and will influence the dynamics of the low order modes.

A. Experimental derivation of dynamics

To investigate the dynamics of the loaded piezoelectric tube, a laser vibrometer (OFV-5000 with OFV-511 sensor and VD-02 decoder, Polytec, Waldbronn, Germany) was used to measure the velocity at the center of the sample disk. The piezoelectric tube was excited using a set of five independent piezo amplifiers.

1) Dynamics of full tube: The frequency response of the full tube was measured before and after cutting of the electrode. The results, shown in Fig. 6 indicate that the dynamical behavior of the tube after cutting is different from the one before cutting. The first two modes shift down by 17% and the third mode by 30% possibly due to damage caused to the piezoelectric material during electrode removal. More importantly, the second mode is now close to the first and second anti-resonance and is therefore less pronounced.

Comparing the results to the model shown in Fig. 1 it is clear that the modes occur at a much lower frequency than expected. The first mode shown the model is 16.7 KHz, while the first measured mode shown in Fig. 6 occurs at 7.5 kHz. The difference in the result can in part be attributed to

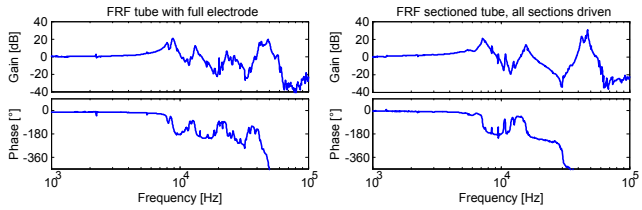

Fig. 6. FRF of loaded piezoelectric actuator, before (left) and after sectioning of the electrodes (right).

the dynamics of the load. Also the contact stiffness between mount and actuator and between the actuator and load will not be infinite because the top and bottom of the piezoelectric tube is not perfectly flat. As a result, the first resonant mode will shift to a lower frequency.

2) Dynamics of sectioned tube: The dynamics of the section tube when the sections are driven independently are shown in Fig. 7. To verify if the model can be used to derive the modal gains, the results of the separate sections were added up and compared to a response measured while driving all tube sections in parallel using the same gain. In Fig. 7 it is shown that results match very well for the first three resonant modes but show a deviation between the third and higher order modes.

For the purpose of modal actuation the second mode has already a small contribution to the dynamics and can in this case be ignored. Focusing on the dynamics of the first and the third mode it is clear that with exception of the first channel, all sections have an anti resonance between the first and third mode. As a result, the mode shapes of the first and second mode of channel 2-5 have the same sign which allows the application of a gain set with 4 positive gains allowing optimization of the static gain.

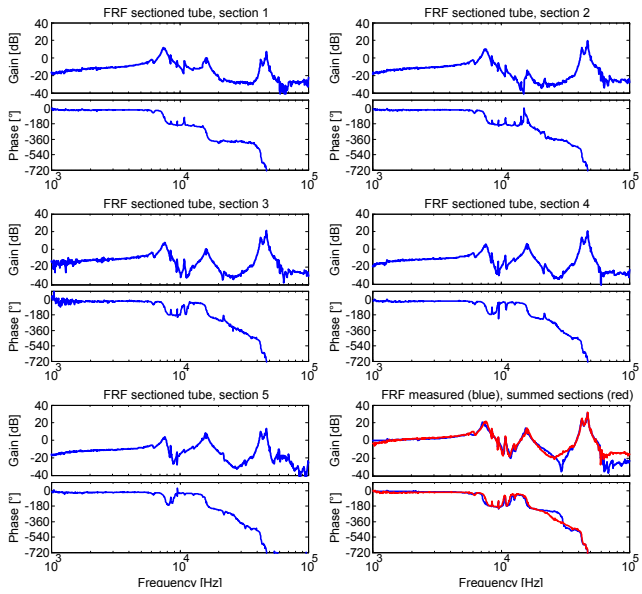

Fig. 7. Measured FRF of sectioned actuator.

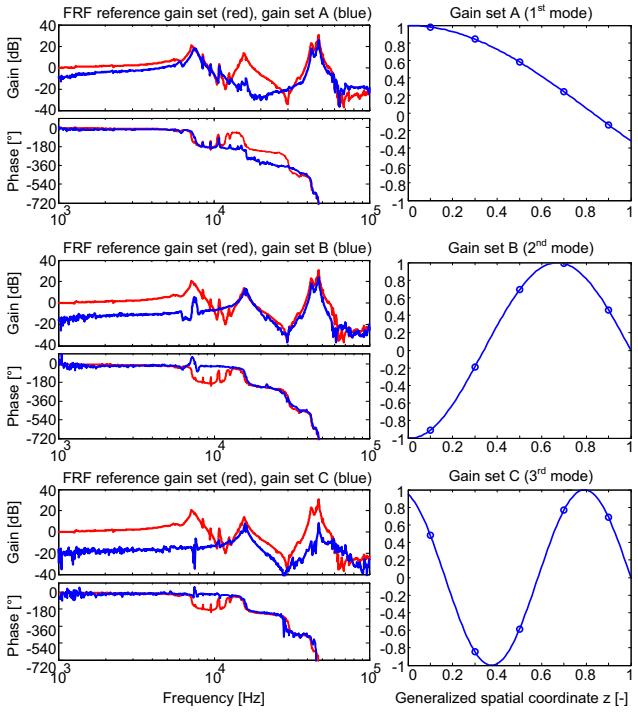

Fig. 8. FRF of piezoelectric tube with section gains set to 1 (red) and section gains set to modal gains of first, second and third mode (blue).

B. Application of modal actuation

Using a set of pre-amplifiers, a modal actuator was constructed using three gain sets (A,B and C in Fig. 8). The results indicate that modal actuation can be used to suppress the first or the third mode. Using the first gain set (A) shown in Fig. 8, the third mode is suppressed significantly but the phase drops at the location of the peak. This effect may be caused by phase differences in the separate amplifier channels which could be improved by further tuning.

The gain set for the second mode (B) reduces the first mode but leaves some gain peaking and does not affect the fourth mode. Using the third order mode shape (C) a better result is obtained. The gain set for the second and third mode have the disadvantage of a reduced static range when compared to the gain set based on the first mode (A).

In summary Fig. 7 & 8 demonstrate experimentally, the ability to apply modal actuation using a set of tuned gains which is in agreement with the theoretical results.

IV. CONCLUSIONS AND FUTURE WORKS

In this paper it is shown that modal actuation can be used to shape the dynamics of a loaded piezoelectric tube scanner by shifting the anti resonances towards the resonant modes.

Varying boundary conditions in the form of changing load conditions affect the mode shapes and the frequency where the resonant modes occur. As a result, a modal actuator based on a gain set optimized for a specific load requires re-tuning.

The use of a sectioned electrode in combination with a set of amplifiers with selectable gains enable the tuning of the modal actuator. The section gains can be tuned using a function resembling the first mode of the axial dynamics, which allows tuning with a limited set of parameters. Furthermore, tuning with a function resembling the first mode enables modal actuation with a minimum loss of static gain.

Future work will focus on increasing the accuracy of the model by using shell theory or finite element modeling and on utilizing modal actuation to optimize the controllability of the system by avoiding excitation of resonant modes at frequencies close to the controller bandwidth.

REFERENCES

[1] G. Binning, C.F. Quate and C. Gerber, Atomic force microscope, *Phys. Rev. Lett* 56(9), pp. 930-33, 1986.

[2] D.Y. Abramovitch, S.B. Andersson, L.Y. Pao and G. Schitter, A Tutorial on the mechanisms, dynamics, and control of atomic force microscopes, *Proc. Amer. Ctrl. Conf.*, July 2007.

[3] J.H. Kindt, G.E. Fantner, J.A. Cutroni and P.K. Hansma, Rigid design of fast scanning probe microscopes using finite element analysis, *Ultramicroscopy*, 100 , pp. 259-65, 2004

[4] G. Schitter, K.J. Åström, B.E. DeMartini, P.J. Thurner, K.L. Turner and P.K. Hansma, Design and modeling of a high-speed AFM-scanner, *IEEE Trans. Control Syst. Technol.*, 15(5), pp. 906-15, 2007.

[5] T. Ando, N. Kodera, E. Takai, D. Maruyama, K. Saito and A. Toda, A high-speed atomic force microscope for studying biological macromolecules, *PNAS* 98(22),pp 12468-72, 2001

[6] G. Schitter, F. Allgöwer and A. Stemmer, A new control strategy for high-speed atomic force microscopy, *Nanotechnology*, 15, pp 10814, 2004

[7] A. Sebastian, S. Salapaka, Design methodologies for robust nano-positioning,*IEEE Trans. Ctrl. Syst. Technol.*, 13(6), pp. 868-76, 2005

[8] N. Kodera, M. Sakashita and T. Ando, Dynamic proportional-integral-differential controller for high-speed atomic force microscopy, *Rev. Sci. Instrum.*, 77, pp. 083704, 2006.

[9] A.J. Fleming and S.O.R Moheimani, Sensorless vibration suppression and scan compensation for piezoelectric tube nanopositioners, *IEEE Trans. Control Syst. Technol.*, 14(1), 2006.

[10] D.Y. Abramovitch, S. Hoen and R. Workman, Semi-automatic tuning of PID gains for atomic force microscopes, *Amer. Ctrl. Conf.*, 2008

[11] M.J. Balas, Active control of flexible systems, J*ournal of Optimization Theory and Applications*, Vol. 25(3), pp. 415-36, 1978

[12] L. Meirovitch, H. Baruh, On the problem of observation spillover in self-adjoint distributed-parameter systems, *J. of Optim. Theory and Appl.*, Vol. 39(2), pp. 269-91, 1983

[13] L. Meirovitch, H. Baruh, Control of Self-Adjoint Distributed-Parameter Systems, *J. of Guid. and Ctrl.*, Vol. 5(1), pp 2053-60, 1982

[14] C.K. Lee,F.C. Moon, Modal Sensors/Actuators, *Journal of Applied Mechanics*, Vol. 57, pp. 434, 1990

[15] A. Preumont, A. Franois, P. De Man, V. Piefort, Spatial filters in structural control, *J. of Sound and Vib.*, Vol 265(1), pp. 61-79, 2003

[16] A. Preumont, A. Franois, P. De Man, N. Loix, K. Henrioulle, Distributed sensors with piezoelectric films in design of spatial filters for structural control, *J. of Sound and Vib.*, Vol. 282(3-5), pp. 701-12, 2005

[17] S. A. Collins, D. W. Miller, A. H. Von Flotow, Distributed Sensors as Spatial Filters in Active Structural Control, *J. of Sound and Vib.*, vol. 173(4), 1994, pp. 471501.

[18] L. Meirovitch, H. Baruh, The implementation of modal filters for control of structures, *J. Guid. Ctrl. and Dyn.*, Vol. 8(6), pp 707-16, 1985

[19] H. J. M. T. A. Adriaens, W. L. de Koning and R. Banning, Modeling piezoelectric actuators, *IEEE/ASME Trans. Mechatron.*, 5(4), pp. 331-41, 2000.

[20] T. Ohara and K. Youcef-Toumi, Dynamics and control of piezotube actuators for subnanometerprecision applications, *Proc. Amer. Ctrl. Conf.*, 5, pp. 3808-12, 1995.

[21] Blevins, R, *Formulas for Natural Frequency and Mode Shape*, Krieger Publishing Company, 2001, ISBN 1-5724-184-6.

[22] Meirovitch L, *Fundamentals of Vibrations*, McGraw-Hill 2001.